IAI Journals.ASM.org

Klebsiella pneumoniae Induces an Inflammatory Response in an *In Vitro* Model of Blood-Retinal Barrier

C. Motta,[a] M. Salmeri,[b] C. D. Anfuso,[a] A. Amodeo,[b] M. Scalia,[c] M. A. Toscano,[b] G. Giurdanella,[a] M. Alberghina,[a] G. Lupo[a]

Department of Clinical and Molecular Biomedicine, University of Catania, Catania, Italy[a]; Department of Bio-Medical Science, University of Catania, Catania, Italy[b]; Department G. F. Ingrassia, Unit of General and Cellular Biology and Molecular Genetics G. Sichel, University of Catania, Catania, Italy[c]

***Klebsiella pneumoniae* has become an important pathogen in recent years. Although most cases of *K. pneumoniae* endogenous endophthalmitis occur via hematogenous spread, it is not yet clear which microbial and host factors are responsible for the ability of *K. pneumoniae* to cross the blood-retinal barrier (BRB). In the present study, we show that in an *in vitro* model of BRB based on coculturing primary bovine retinal endothelial cells (BREC) and primary bovine retinal pericytes (BRPC), *K. pneumoniae* infection determines changes of transendothelial electrical resistance (TEER) and permeability to sodium fluorescein. In the coculture model, bacteria are able to stimulate the enzyme activities of endothelial cytosolic and Ca^{2+}-independent phospholipase A_2s (cPLA$_2$ and iPLA$_2$). These results were confirmed by the incremental expression of cPLA$_2$, iPLA$_2$, cyclo-oxygenase-1 (COX1), and COX2 in BREC, as well as by cPLA$_2$ phosphorylation. In supernatants of *K. pneumoniae*-stimulated cocultures, increases in prostaglandin E_2 (PGE_2), interleukin-6 (IL-6), IL-8, and vascular endothelial growth factor (VEGF) production were found. Incubation with *K. pneumoniae* in the presence of arachidonoyl trifluoromethyl ketone ($AACOCF_3$) or bromoenol lactone (BEL) caused decreased PGE_2 and VEGF release. Scanning electron microscopy and transmission electron microscopy images of BREC and BRPC showed adhesion of *K. pneumoniae* to the cells, but no invasion occurred. *K. pneumoniae* infection also produced reductions in pericyte numbers; transfection of BREC cocultured with BRPC and of human retinal endothelial cells (HREC) cocultured with human retinal pericytes (HRPC) with small interfering RNAs (siRNAs) targeted to cPLA$_2$ and iPLA$_2$ restored the pericyte numbers and the TEER and permeability values. Our results show the proinflammatory effect of *K. pneumoniae* on BREC, suggest a possible mechanism by which BREC and BRPC react to the *K. pneumoniae* infection, and may provide physicians and patients with new ways of fighting blinding diseases.**

Endogenous bacterial endophthalmitis (EBE), a potentially blinding ocular emergency, develops secondary to hematogenous spread of microorganisms from a septic focus. It is associated with underlying immunosuppressive conditions, including diabetes mellitus, HIV infection, indwelling catheters, cardiac disease, renal insufficiency, malignancy, or immunosuppressive therapy (1–5). Moreover, EBE is a rare but potential complication of neonatal sepsis (6). EBE occurs when the eye is seeded via the bloodstream. Patients usually have symptoms from their underlying systemic infection but sometimes present only with eye symptoms. In panophthalmitis, infection spreads from the globe of the eye to the adjacent soft tissues of the orbit. Most cases of endophthalmitis present acutely, within hours to a few days of symptoms. These cases are medical emergencies, as delay in treatment may result in permanent vision loss (7). Common pathogens in Western countries include *Streptococcus aureus* (25% of cases), streptococci (30 to 50%; primarily *Streptococcus pneumoniae*, *Streptococcus milleri* group, and group A and B streptococci), and Gram-negative bacilli, such as *Escherichia coli* (30%). In Asia, *Klebsiella pneumoniae* causes the majority of cases. Treatment of the underlying source of bacteremia with systemic antibiotics is necessary, but this will not effectively treat the endophthalmitis: intravitreal antibiotics and, usually, a vitrectomy are necessary (8–10). *K. pneumoniae* typically expresses smooth lipopolysaccharide (LPS), with O-antigen polysaccharide (O-PS) and antigenic capsular polysaccharide (K-PS) on its surface; both antigens, O-PS and K-PS, contribute to the pathogenesis of this species (11).

K. pneumoniae has become an important pathogen in recent years. Invasive strains causing pyogenic liver abscesses and other soft tissue abscesses have been reported with increasing frequency. Recently, infections have been reported in the United States, Europe, the Middle East, and Australia (12–16). These reports suggest that, rather than being confined to Taiwan, endogenous endophthalmitis secondary to a liver abscess due to *K. pneumoniae* is becoming a global problem. Of importance was the discovery of the mucoviscosity-associated gene A (called *magA* and later designated *wzy*-K1) in screens of invasive liver isolates (17). A recent study demonstrated that both whole live *K. pneumoniae* cells and *K. pneumoniae* LPS exert strong proinflammatory effects on retinal pigmented epithelial cells, consistent with clinical manifestations of endogenous endophthalmitis (18). Despite treatment, most patients with *K. pneumoniae* EBE lose useful vision. The reason for the poor outcome may depend on the limited knowledge of the pathogenesis and pathophysiology of the disease. Although most cases of *K. pneumoniae* EBE occur via hematogenous spread, it is not yet clear which microbial and host factors are responsible for the ability of *K. pneumoniae* to cross the blood-retinal barrier (BRB).

The BRB is essential to maintaining the eye as a privileged site,

Received 12 July 2013 **Returned for modification** 6 September 2013
Accepted 2 December 2013
Published ahead of print 9 December 2013
Editor: B. A. McCormick
Address correspondence to G. Lupo, lupogab@unict.it.
C. Motta, M. Salmeri, and M. Scalia contributed equally to this article.

doi:10.1128/IAI.00843-13

as well as for normal visual function, and the most frequent and relevant ocular diseases are directly associated with alterations of the BRB (19). Under physiological conditions, the intercellular spaces between retinal endothelial cells that form the BRB are sealed by elaborate tight junctions and the cells themselves lack fenestrations and have few pinocytotic vesicles. These features of the BRB, which are comparable to those of the BRB endothelium, result in high transendothelial electrical resistance (TEER) and restricted paracellular permeability (20). The retinal continuous endothelium forms the main structure of the BRB and rests on a basal lamina that is covered by the processes of astrocytes, Müller cells, and pericytes (blood-retinal pericytes [BRPC]s); the latter are encased in the basal lamina, in close contact with the blood retinal endothelial cells (BREC). BRPC, astrocytes, and Müller cells are considered to influence the activity of the BREC and BRB by transmitting regulatory signals to BREC, indicating changes in the microenvironment of the retinal neuronal circuitry (21). In particular, BRPC are uniquely positioned within the microvessels to serve as vital integrators, coordinators, and effectors of many neurovascular functions, including angiogenesis, barrier formation and maintenance, vascular stability, angioarchitecture, and regulation of capillary blood flow (22). The recruitment of pericytes to a vascular tube of endothelial cells is closely associated with the formation of tight junctions in developing retinal vessels (23). Although normally not in contact with blood flow due to their subendothelial location, after vascular injury, BRPC may participate in intravascular processes like thrombosis and hemostasis (24). It is recognized that BRPC loss is a typical sign of early microangiopathy of the diabetic retina (25). The role of BRPC in the maintenance of the BRB during EBE is still to be elucidated. Our study places the vital cross-talk between BREC and BRPC at the center of injury responses in *K. pneumoniae* EBE.

Arachidonic acid (AA) is liberated from phospholipids by the action of different isoforms of phospholipase A_2s (PLA_2s) and converted to prostaglandins (PGs) or leukotrienes (LTs) by the action of cyclo-oxygenase (COX) and 5-lipoxygenase, respectively. Cytosolic PLA_2 ($cPLA_2$), Ca^{2+}-independent intracellular PLA_2 ($iPLA_2$), and Ca^{2+}-dependent secretory PLA_2 ($sPLA_2$) differ from each other in terms of substrate specificity, Ca^{2+} requirement, lipid modification, translocation to cellular membranes, and AA release (26).

Several studies have shown that bacterial infection triggers an endothelial proinflammatory response, including the secretion of cytokines that are responsible for the activation of inflammatory cells and facilitate the recruitment of leukocytes to the site of injury. Interleukin-6 (IL-6) and IL-8 are necessary for initiating an effective endothelial response against infection (27, 28).

It has been demonstrated that the systemic delivery of vascular endothelial growth factor (VEGF) ablates pericytes from the mature retinal vasculature through the VEGF receptor-1 (VEGFR1)-mediated signaling pathway, leading to increased vascular leakage, and the blockade of VEGFR-1 significantly restores BRPC saturation in mature vessels (29). Our previous studies have shown the role of PLA_2s, prostaglandins, and VEGF release in governing the penetration of *Escherichia coli* into the brain (30, 31). Recognizing the importance of retinal endothelial cells and pericytes as a barrier to endogenous infectious agents in human endophthalmitis, in this study, we investigated the effects of *K. pneumoniae* on these cells. In the present paper, we show that, in an *in vitro* model of BRB, based on coculturing BREC and BRPC, *K. pneumoniae* invasion is associated with decreased TEER and increased permeability of the BRB due to the loss of BRPC. Furthermore, we present evidence that endothelial PLA_2s plays a significant role in these events. These findings suggest a possible mechanism by which BREC and BRPC react to the *K. pneumoniae* infection.

MATERIALS AND METHODS

All reagents and antibodies were purchased from Sigma (St. Louis, MO) or E. Merck (Darmstadt, Germany) unless otherwise indicated. Phospholipase A_2 inhibitors, arachidonoyl trifluoromethyl ketone ($AACOCF_3$), and bromoenol lactone (BEL) were from Calbiochem (La Jolla, CA). NS-398 (*N*-[2-(cyclohexyloxy)-4-nitrophenyl]-methanesulfonamide), which is a selective cyclo-oxygenase-2 inhibitor, and rabbit anti-$iPLA_2$ polyclonal antibody were from Cayman Chemical Co. (Ann Arbor, MI). Rabbit polyclonal anti-von Willebrandt factor antibody and mouse monoclonal anti-$cPLA_2$, anti-α-actin, anti-COX-1, anti-COX-2, and anti-glyceraldehyde-3-phosphate dehydrogenase (GAPDH) antibodies were purchased from Santa Cruz Biotechnology, Inc. (CA).

Cell cultures. Primary bovine retina microvascular endothelial cells (BREC) were purchased from European Collection of Cell Cultures (ECACC) and were fed with Ham's F-10 medium as previously described (32). Primary human retina microvascular endothelial cells (HREC) and human retina microvascular pericytes (HRPC) were purchased from Innoprot and were maintained in basal medium supplemented with 10% fetal bovine serum (FBS), 100 U/ml penicillin, 100 μg/ml streptomycin, and endothelial cell growth supplement (ECGS). Pure microvessel bovine pericyte cultures were prepared from bovine retinas, as previously described (33). The isolated cells were then cultured in Dulbecco's modified Eagle's medium (DMEM) supplemented with 10% FBS, 100 U/ml penicillin, and 100 μg/ml streptomycin. Morphological changes and cell viability were determined with the MTT [3-(4,5-dimethyl-2-thiazolyl)-2,5-diphenyl-2H-tetrazolium bromide] test (34). Pericytes were characterized by their large size and branched morphology, positive immunostaining for α-smooth muscle actin and NG2 chondroitin sulfate proteoglycan, and absence of von Willebrand factor and glial fibrillary acidic protein (GFAP) staining.

Construction of *in vitro* BRB model. Inserts (Transwells; Corning Inc., Corning, NY), were coated on the top and bottom with a 2 mg/ml solution of rat tail collagen containing 10-fold concentrated DMEM plus 0.3 M NaOH. The coating was dried for 1 h at 37°C and was rinsed twice with water and once with Ca^{2+}- and Mg^{2+}-free phosphate-buffered saline (PBS) before being placed in complete medium. To construct an *in vitro* model of BRB based on direct contact of cells, BRPC or HRPC were first plated on the outside of the polycarbonate membrane (2×10^4 cells/cm^2) of the Transwell inserts (6-well type with 0.4-μm or 3.0-μm pore size) and placed upside down in the well culture plate. After BRPC or HRPC had adhered, the Transwells were inverted and reinserted into 6-well plates, and BREC or HREC were seeded on the top surface of the insert (2×10^4 cells/cm^2) (see Fig. 1). After coincubation for 24 h, the medium was discarded and replaced with fresh medium (50% DMEM plus 50% F-10 HAM's medium containing 10% FBS); under these conditions, the *in vitro* BRB model was established within 3 days after cell seeding, to obtain the full confluence. As negative controls for barrier integrity studies, BREC and BRPC in monocultures, which do not form the barrier, were cultured on the respective inserts.

Preparation of *K. pneumoniae*. *K. pneumoniae* strain ATCC 43816 serotype 2 culture was grown in Luria-Bertani (LB) medium (Difco, Sparks, MD) for 14 h at 37°C. The culture was centrifuged at 3,000 rpm for 10 min, and the supernatant discarded. The bacterial pellet was washed with PBS (Gibco, Invitrogen, Carlsbad, CA) and serially diluted to the desired concentration. The density of bacteria was measured by enumerating the number of CFU on LB agar plates (Difco).

Coculture infection with *K. pneumoniae*. Cocultures were grown to confluence. FBS-containing medium was removed, and serum-free medium was added to the cocultures 4 h before infection with *K. pneumoniae*

(10^7 CFU/well). After infection for 60 min with bacteria, the cocultures were washed three times with PBS, and endothelial cells and pericytes were collected separately by trypsinization. *K. pneumoniae*-free cocultures served as uninfected controls.

Fluorescence laser scanning confocal microscopy. To characterize BREC and BRPC in coculture, immunocytochemistry was performed with a confocal fluorescence microscope. After incubation in coculture, BREC or BRPC grown on one side of the filter were removed by rubbing it on filter paper to leave only one cell type. The filters with BREC or BRPC were washed, fixed by adding 4% paraformaldehyde in PBS, and processed for immunocytochemistry as previously described (35), using the following antibodies to highlight cell architecture: mouse anti-α-actin monoclonal antibody (BRPC marker), or rabbit anti-von Willebrand factor polyclonal antibody (BREC marker). All primary antibodies were used in a dilution of 1:100. As the secondary antibody, green fluorescence-labeled fluorescein isothiocyanate (FITC) antibody was used in a dilution of 1:1,000. The distribution of immunocomplexes was observed by confocal immunofluorescence microscopy using an Olympus FV1000 confocal laser scanning microscope. Single lower-power scans were followed by 16 to 22 serial optical sections of randomly chosen cells in four to five fields per coverslip. The average fluorescence (mean ± standard deviation [SD]) intensity (pixel) in individual cell bodies was measured throughout the stack. Each condition was tested on a total of 60 to 80 cells, recovered from at least three coverslips obtained from a least two different cell cultures.

Electron microscopy. For scanning electron microscopy (SEM) preparations, cells grown on the membrane were fixed with 1.5% glutaraldehyde in 0.12 M phosphate buffer (pH 7.5) overnight at 4°C. After being washed with phosphate buffer several times, the membranes of the culture inserts with the cells on the two sides were removed from their support and placed into a 24-well chamber slide and then were postfixed in 1% OsO_4 for 1 h at 4°C. Following washing with distilled water, the cells on the membrane were dehydrated in graded ethanol, critical point dried, and sputtered with a 5-nm gold layer using an Emscope SM 300 (Emscope Laboratories, Ashford, United Kingdom). They were then observed using a Hitachi S-4000 (Hitachi High-Technologies America, Inc., Schaumburg, IL) field emission scanning electron microscope.

For transmission electron microscopy (TEM), after being dehydrated in a graded series of acetone, cells were embedded in Durcupan ACM (Fluka Chemika-Biochemika, Buchs, Switzerland). Ultrathin sections were cut perpendicularly from the membrane using a Reichert Ultracut E microtome and double stained with uranyl acetate and lead citrate. Observations were carried out using a Hitachi H-7000 transmission electron microscope (Hitachi High-Technologies Europe GmbH, Krefeld, Germany).

Evaluation of the barrier integrity. TEER was measured using a Millicell electrical resistance system (ERS) (Millipore). The collagen-treated Transwell inserts were used to measure the background resistance. Values were expressed as $\Omega \times cm^2$ and were calculated by the following formula: (average resistance of experimental wells − average resistance of blank wells) × 0.33 (the area of the Transwell membrane).

To determine the flux of sodium fluorescein (Na-F) across the endothelial monolayer, inserts containing cell cultures were transferred to 12-well plates containing 1.5 ml Ringer-HEPES buffer (136 mM NaCl, 0.9 mM $CaCl_2$, 0.5 mM $MgCl_2$, 2.7 mM KCl, 1.5 mM KH_2PO_4, 10 mM NaH_2PO_4, 25 mM glucose, and 10 mM HEPES, pH 7.4) in the lower or abluminal compartments. In the inserts (luminal compartment), culture medium was replaced by 0.5 ml buffer containing 10 μg/ml Na-F (376 Da). The inserts were transferred at 5, 15, and 30 min to a new well containing Ringer-HEPES buffer. The concentrations of the marker molecule in samples from the upper and lower compartments were determined by using a fluorescence multiwell plate reader (excitation wavelength, 485 nm, and emission wavelength, 535 nm; PerkinElmer). The flux across cell-free inserts was also measured, and the transendothelial permeability coefficient (P_e) was calculated. Permeability measurements of triplicate filters for each culture condition were performed. Transport was expressed as microliters of donor (luminal) compartment volume from which the tracer was completely cleared, as follows: cleared volume (μl) = $\text{concentration}_{\text{abluminal}} \times \text{volume}_{\text{abluminal}} \times \text{concentration}^{-1}{}_{\text{luminal}}$. The average cleared volume was plotted versus time, and the product value for permeability times surface area for the endothelial monolayer (PS_e) was calculated by the following formula: $PS^{-1}{}_{\text{endothelial}} = PS^{-1}{}_{\text{total}} - PS^{-1}{}_{\text{insert}}$. The PS_e divided by the surface area (1 cm^2 for Transwell-12) generated the endothelial permeability coefficient (P_e in 10^{-6} cm/s).

Bacterial invasion and adhesion assays. Invasion of BREC by *K. pneumoniae* in monoculture and in coculture with BRPC was performed as described by Zhu et al. (36). Bacteria (10^7 CFU/well) were added to confluent cells in monoculture or in coculture, and incubations were performed at 37°C for 60 min to allow invasion to occur. The number of intracellular bacteria was determined after incubation with gentamicin (100 μg/ml) for 1 h at 37°C. Cells were washed and lysed with 0.5% Triton X-100. The intracellular bacteria released were enumerated by seeding on LB agar plates. In duplicate experiments, the total cell-associated bacteria were determined as described for invasion, except that the gentamicin step was omitted. The results were expressed as percent invasion [100 × (number of intracellular bacteria recovered)/(number of bacteria inoculated)].

Cell viability. In order to determine the number and viability of cells in BREC-BRPC and HREC-HRPC cocultures after *K. pneumoniae* treatment for 60 min, cells from inserts were trypsinized separately, cell suspensions were mixed with a 0.4% (wt/vol) trypan blue solution, and the number of live cells was determined using a hemocytometer. Cells failing to exclude the dye were considered not viable. Experiments were performed in triplicate and counted 4 times each.

Immunoblotting. The lysates of BREC incubated with *K. pneumoniae* strains for 60 min were prepared for Western blotting as previously described (32). Membranes were incubated with primary antibodies against $cPLA_2$, $iPLA_2$, COX-1, and COX-2 and then with secondary antibodies for 1 h at room temperature.

Phospholipase A_2 assay. BREC and BRPC in mono- or coculture were preincubated for 60 min in culture medium supplemented or not with either 50 μM $AACOCF_3$ or 2.5 μM BEL. The cells were then refed with fresh culture medium containing the inhibitors in the presence or absence of *K. pneumoniae* for 60 min. Controls were performed by incubation of cocultures with inhibitors for 120 min in the absence of bacteria. At the end of the incubations, the cells grown on both sides of the inserts were scraped with a rubber policeman and saved separately; BREC and BRPC were lysed as previously described (35), and equal amounts of cell lysates were incubated in a 96-well plate with the substrate arachidonoyl-thiophosphatidylcholine (ATPC), using a $cPLA_2$ assay kit (Cayman Chemicals Co., Ann Arbor, MI) and following the manufacturer's instructions. For $sPLA_2$ enzyme activity, an $sPLA_2$ enzyme-linked immunosorbent assay (ELISA) kit (Cayman Chemicals Co., Ann Arbor, MI) was used, following the manufacturer's instructions.

The use of BEL on control and bacterial-treated cells allowed us to discriminate between cytosolic and $iPLA_2$ activities. None of these components, used at the concentrations specified below, affected cell viability, as verified by the trypan blue exclusion test. The results for $cPLA_2$ activity were expressed as pmol of ATPC hydrolyzed per minute and per milligram of protein (pmol/min/mg).

Determination of PGE_2 and VEGF production. To determine PGE_2 and VEGF liberation, BREC and BRPC in coculture were preincubated for 60 min in culture medium supplemented or not with 50 μM $AACOCF_3$, 2.5 μM BEL, or 5 μM NS-398. The cells were then refed with fresh culture medium containing the inhibitors in the presence or absence of *K. pneumoniae* for 30 and 60 min. Supernatants were collected, and aliquots were employed for PGE_2 determination using a kit from Cayman Chemicals Co., Ann Arbor, MI. For PGE_2, the detection range was 7.8 to 1,000 pg/ml. Conditioned medium was removed from the Transwells and analyzed for VEGF by ELISA, using a kit from R&D Systems Inc., Minneapolis, MN, as specified by the manufacturer's instructions. For VEGF, the detection

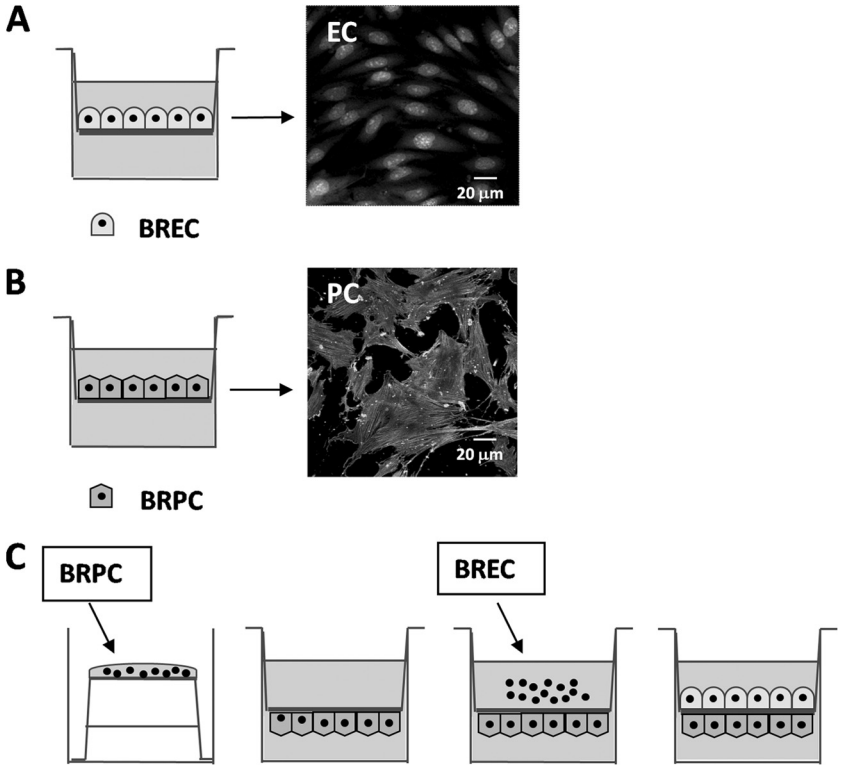

FIG 1 Scheme of Transwell systems for mono- and cocultures of bovine retinal endothelial cells (BREC) and bovine retinal pericytes (BRPC). BREC and BRPC monolayers were grown (A and B); BRPC were seeded on the lower side of the membrane until confluence, and then the BREC were seeded in the upper compartment (C).

range was 20 to 2,500 pg/ml. Each sample from three different experiments was analyzed in triplicate.

Determination of cytokine production. BREC-BRPC cocultures were incubated for 60 min in presence or absence of *K. pneumoniae*. Conditioned medium was removed from the Transwells, and the levels of IL-6 and IL-8 were measured using a commercially available ELISA as specified by the manufacturer's instructions (BD Biosciences). Each sample from three different experiments was analyzed in triplicate.

Transfection of siRNAs. BREC or HREC were transfected with an ON-TARGETplus SMARTpool small interfering RNA (siRNA) duplex obtained from Dharmacon, Inc. (Chicago, IL) to obtain $iPLA_2$ siRNA-transfected BREC ($iPLA_2$ siRNA-BREC), $iPLA_2$ siRNA-HREC, $cPLA_2$ siRNA-BREC, or $cPLA_2$ siRNA-HREC. Two sets of oligonucleotides were used. Set 1 was directed to $iPLA_2$ (GenBank accession number NM_001005560) and had sequences 5′-GGUGUGAGAUGGUCGGUAU-3′, 5′-ACGCUGAGAUGGCCCGAAU-3′, 5′-CAGCAAGGAUCCUCGCUAU-3′, and 5′-CAGAAUGCUUCCAAUCGUA-3′. Set 2 was directed against $cPLA_2$ (GenBank accession number NM_133551) and had sequences 5′-AGAAUUUAGUCCAAUCGAA-3′, 5′-CAUAUCUACACAUGCGAAA-3′, 5′-CAGAUGAAUUUGAACGAAU-3′, and 5′-GCGGAAAGAGAGUACCAAA-3′. A scrambled siRNA control comprised of a nontargeting siRNA pool from Dharmacon, Inc., was used to obtain nontargeting siRNA-transfected BREC (nt-siRNA-BREC) or nt-siRNA-HREC. Transfection of siRNA was performed using Interferin reagent (Dharmacon) according to the manufacturer's protocol, as previously reported (32). The efficiency of transfection (50 nmol/ml siRNAs) was evaluated by using siGLO green transfection indicator (Dharmacon). Western blot analyses were used to confirm the reduction of the protein target. These data were confirmed by determining $cPLA_2$ and $iPLA_2$ enzymatic activity, which was almost undetectable in siRNA-treated samples (data not shown). Control BREC or HREC (transfected with empty vector), nt-siRNA-BREC or nt-siRNA-HREC, $cPLA_2$ siRNA-BREC or $cPLA_2$ siRNA-HREC, and $iPLA_2$ siRNA-BREC or $iPLA_2$ siRNA HREC were cultured until confluence on the Transwell insert in which BRPC or HRPC, respectively, were grown on the lower side of the membrane. After reaching confluence, the cocultures were infected with *K. pneumoniae* for 60 min. In order to determine the number and viability of BREC, BRPC, HREC, and HRPC in coculture, cells from inserts were trypsinized separately, cell suspensions were mixed with a 0.4% (wt/vol) trypan blue solution, and the number of live cells was determined using a hemocytometer.

Statistical analysis. Statistical significance between two groups was analyzed by Student's test. One-way analysis of variance (ANOVA), followed by Tukey's *post hoc* test, was used to compare the means for the multiple groups. P values of <0.05 were considered statistically significant.

RESULTS

TEER and permeability to sodium fluorescein in BREC-BRPC cocultures. The BRB model used in the present study is shown in Fig. 1. To highlight the cell phenotype and for immunological characterization, BREC were incubated with rabbit anti-von Willebrand factor polyclonal antibody (BREC marker) (Fig. 1A) and BRPC were incubated with mouse anti-α-actin monoclonal antibody (BRPC marker) (Fig. 1B). The distribution of immunocomplexes, observed by confocal immunofluorescence microscopy, showed an elongated spindle shape for BREC and an irregular large stellate shape for BRPC. The BRB model, used in all experiments with confluent cells, was characterized by measuring TEER and sodium fluorescein flux across BREC in monoculture and in

TABLE 1 Evaluation of the barrier integrity in BREC and BRPC mono- and cocultures with and without *K. pneumoniae*[a]

Culture	Mean value ± SEM[b]	
	TEER (ω × cm^2)	P_e (10^{-6} cm/s)
Monoculture		
BREC	83 ± 9.4	8.7 ± 0.9
BREC + *K. pneumoniae*	74 ± 6.5	10.2 ± 0.7
Coculture		
BREC-BRPC	289 ± 26.3*	2.9 ± 0.3*
BREC-BRPC + *K. pneumoniae*	98 ± 7.8†	7.9 ± 0.6†

[a] TEER and permeability to sodium fluorescein were determined in bovine retinal microvascular endothelial cells (BREC) in mono- and coculture with bovine retinal microvascular pericytes (BRPC) in the absence or presence of *K. pneumoniae*. Cocultures were incubated in the absence or presence of *K. pneumoniae* (10^7 CFU/well) for 60 min, and measurements of TEER and cell permeability to sodium fluorescein of BREC were performed as described in Materials and Methods. For TEER measurements, values were calculated by the following formula: (average resistance of experimental wells − average resistance of blank cells) × 0.33 (the area of the Transwell membrane). For sodium fluorescein determination, flux across cell-free inserts was measured and the transendothelial permeability coefficient (P_e) was calculated.
[b] Values are from six independent experiments ($n = 6$). ANOVA and the Tukey posttest were used to compare TEER or permeability measurements under the four different experimental conditions. *, $P < 0.05$ versus BREC; †, $P < 0.05$ versus uninfected BREC-BRPC cocultures.

TABLE 2 PLA_2 activity in BREC and BRPC in mono- and cocultures stimulated and not stimulated by *K. pneumoniae*[a]

Culture and inhibitor	Mean PLA_2 activity (pmol/min/mg) ± SEM in[b]:	
	Control cells	Cells + *K. pneumoniae*
Monoculture		
BREC	22.3 ± 1.8	38.3 ± 2.6†
BREC + $AACOCF_3$	16.1 ± 1.3*	19.5 ± 1.7*
BREC + BEL	18.4 ± 1.5*	25.2 ± 1.8*
BRPC	15.6 ± 1.4	18.1 ± 1.2
BRPC + $AACOCF_3$	11.2 ± 0.9*	12.6 ± 1.3*
BRPC + BEL	12.5 ± 0.5*	13.1 ± 0.7*
Coculture		
BREC	31.6 ± 2.8	93.4 ± 7.8†
BREC + $AACOCF_3$	20.1 ± 1.7*	25.4 ± 2.9*
BREC + BEL	23.5 ± 1.9*	28.1 ± 2.6*
BRPC	14.3 ± 1.2	17.2 ± 1.5
BRPC + $AACOCF_3$	9.9 ± 1.0*	10.8 ± 1.1*
BRPC + BEL	11.0 ± 0.8*	13.0 ± 1.5*

[a] All incubations were performed at 37°C in the absence (control) or presence of *K. pneumoniae* (10^7 CFU/well) for 60 min with or without 50 μM $AACOCF_3$ or 2.5 μM BEL. Inhibitors were added to the culture medium 60 min before *K. pneumoniae* was added. PLA_2 activity was measured following enzymatic hydrolysis of arachidonoyl thiophosphatidylcholine (ATPC).
[b] Values are from three independent experiments ($n = 3$). ANOVA and the Tukey posttest were used to compare enzyme activities measurements under the 24 different experimental conditions. *, $P < 0.05$ versus the same group without inhibitors; †, $P < 0.05$ versus control BREC.

coculture with BRPC (Table 1). Coculture showed high values of TEER and very low permeability to sodium fluorescein in comparison with the values in BREC monoculture. Very similar results in repeated experiments indicated the reproducibility of the model. Incubation for 60 min with *K. pneumoniae* (10^7 CFU/well) caused a significant TEER reduction (about 2.9-fold) and an increased permeability (about 2.7-fold) compared to the values for BREC-BRPC control cocultures.

***K. pneumoniae* stimulates phospholipase A_2 activities, PGE_2 production, and VEGF, IL-6, and IL-8 release.** As reported in Table 2, in *K. pneumoniae*-stimulated BREC in mono- and coculture, PLA_2 activity was strongly activated (about 2.6-fold in mono- and 2.9-fold in cocultures) compared with the PLA_2 activity in the control (uninfected) BREC; this result was unlike the result for BRPC, in which it was not stimulated. In *K. pneumoniae*-treated BREC monocultures, the presence for 120 min (preincubation of 60 min followed by infection for 60 min in the presence of bacteria) of 50 μM $AACOCF_3$ ($cPLA_2$ and $iPLA_2$ activity inhibitor) or 2.5 μM BEL ($iPLA_2$ inhibitor) caused decreases of 62% and 51%, respectively; in control BREC monocultures, $AACOCF_3$ and BEL caused decreases of enzyme activity of 28% and 17%, respectively. In control BRPC monocultures, $AACOCF_3$ caused decreases of 28% and 20%, respectively, and in *K. pneumoniae*-stimulated BRPC monocultures, the inhibitors caused decreases of 30% and 20%, respectively.

In control BREC grown in coculture with BRPC, $AACOCF_3$ reduced enzymatic activity by 36% and BEL by 25%, and after *K. pneumoniae* treatment in the presence of the inhibitors, enzymatic activity decreased by about 73% and 70% in BREC cocultures. Moreover, $AACOCF_3$ and BEL decreased PLA_2 activity in control BRPC by 31% and by 23%, respectively, and in *K. pneumoniae*-treated BRPC, they decreased PLA_2 activity by about 37% and 24%, respectively. The incubation with BEL allowed us to discriminate between the contributions of $cPLA_2$ and $iPLA_2$ activities. Interestingly, the significant decrease in BREC enzyme activity in the presence of BEL suggests a greater contribution of $iPLA_2$ in mediating AA release by *K. pneumoniae*-stimulated cells. Specific activity in *K. pneumoniae* lysates was undetectable (data not shown).

PGE_2 production was detected in supernatants of BREC or BRPC in mono- and coculture. As shown in Table 3, a 3.0-fold increase was observed in BREC monocultures after *K. pneumoniae* treatment, compared to the PGE_2 production in the respective control (no treatment). In control BREC monocultures, the presence of 50 μM $AACOCF_3$ or 2.5 μM BEL caused decreases of 29% and of 18%, respectively. Incubation of BREC monocultures with *K. pneumoniae* in the presence of $AACOCF_3$ or BEL decreased PGE_2 production by 68% and 66%, respectively. The contribution to PGE_2 production from *K. pneumoniae*-treated BRPC monocultures was negligible.

The production of PGs from BREC in great amounts during *K. pneumoniae* infection highlights the principal endothelial role in BRB disruption.

The PGE_2 production in untreated cocultures was about 2.4- to 2.7-fold higher than that of the respective monocultures. In *K. pneumoniae*-treated cocultures, prostaglandin production was higher than the predicted sum of that produced by BREC and BRPC monocultures. When BREC-BRPC cocultures were treated with *K. pneumoniae*, the PGE_2 production increased by 3.4-fold in comparison with that in the respective untreated cocultures. Furthermore, in the supernatants of *K. pneumoniae*-stimulated cocultures incubated in the presence of PLA_2 inhibitor $AACOCF_3$ or BEL, the PGE_2 levels decreased by about 70% and 69%, respectively, and the decreases were about 28% and 22%, respectively, for untreated cocultures.

TABLE 3 Prostaglandin production in BREC and BRPC in mono- and cocultures stimulated and not stimulated by *K. pneumoniae*[a]

Culture and inhibitor	Mean amt of PGE_2 (pg/ml) ± SEM in[b]: Control cells	Cells + *K. pneumoniae*
Monoculture		
BREC	86 ± 8.1	261 ± 22.4†
BREC + $AACOCF_3$	61 ± 6.9*	84 ± 7.7*
BREC + BEL	70 ± 7.1*	87 ± 6.9*
BRPC	78 ± 6.5	80 ± 7.8
BRPC + $AACOCF_3$	55 ± 3.8*	58 ± 4.5*
BRPC + BEL	58 ± 5.6*	61 ± 5.8*
Coculture		
BREC-BRPC	212 ± 18.7§	732 ± 54.1‡
BREC-BRPC + $AACOCF_3$	153 ± 16.6*	218 ± 17.5*
BREC-BRPC + BEL	164 ± 17.4*	224 ± 15.6*

[a] Cell culture supernatants from mono- and cocultures in the absence (control) and presence of *K. pneumoniae* (10^7 CFU/well for 60 min) and with or without 50 μM $AACOCF_3$ or 2.5 μM BEL were assayed for PGE_2 production. Inhibitors were added to the culture medium 60 min before *K. pneumoniae* was added.
[b] Values are from three independent experiments ($n = 3$). ANOVA and the Tukey posttest were used to compare PGE_2 production under the 18 different experimental conditions. *, $P < 0.05$ versus the same group without inhibitors; †, $P < 0.05$ versus control BREC; ‡, $P < 0.05$ versus control BREC-BRPC cocultures; §, $P < 0.05$ versus monocultures.

BREC monocultures produced moderate amounts of VEGFA (referred to here as VEGF) protein in the conditioned medium (27.8 ± 1.5 [mean ± SD]), and incubation for 60 min with *K. pneumoniae* led to a 2.5-fold increase in the release of VEGFA (Table 4). BRPC monocultures released physiologically higher

TABLE 4 VEGFA determination in BREC and BRPC in mono- and cocultures stimulated and not stimulated by *K. pneumoniae*[a]

Culture and inhibitor	Mean amt of VEGFA (pg/ml) ± SEM in[b]: Control cells	Cells + *K. pneumoniae*
Monoculture		
BREC	27.8 ± 1.5	70.4 7.5†
BREC + $AACOCF_3$	15.1 ± 1.2*	21.1 ± 2.3*
BREC + BEL	18.5 ± 1.7*	23.2 ± 3.4*
BREC + NS-398	14.8 ± 1.1*	20.4 ± 2.3*
BRPC	44.8 ± 4.2†	46.3 ± 3.9
BRPC + $AACOCF_3$	34.6 ± 2.9*	35.5 ± 3.6*
BRPC + BEL	36.1 ± 2.7*	37.4 ± 4.2*
BRPC + NS-398	33.7 ± 3.1*	29.5 ± 3.1*
Coculture		
BREC-BRPC	118.4 ± 9.3§	346.4 ± 32.2‡
BREC-BRPC + $AACOCF_3$	85.1 ± 7.2*	88.1 ± 8.4*
BREC-BRPC + BEL	88.7 ± 8.1*	93.7 ± 10.4*
BREC-BRPC + NS-398	85.2 ± 7.7*	86.3 ± 7.3*

[a] Cell culture supernatants from mono- and cocultures in the absence (control) and presence of *K. pneumoniae* (10^7 CFU/well for 60 min) and with or without 50 μM $AACOCF_3$, 2.5 μM BEL, or 5 μM NS-398 were assayed for VEGF release. Inhibitors were added to the culture medium 60 min before *K. pneumoniae* was added.
[b] Values are from three independent experiments ($n = 3$). ANOVA and the Tukey posttest were used to compare VEGF release under the 24 different experimental conditions. *, $P < 0.05$ versus the same group without inhibitors; †, $P < 0.05$ versus control BREC; ‡, $P < 0.05$ versus control BREC-BRPC cocultures; §, $P < 0.05$ versus monocultures.

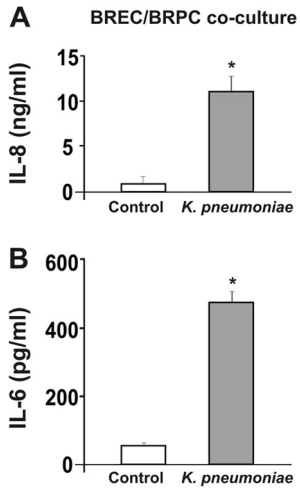

FIG 2 IL-6 (B) and IL-8 (A) production in BREC-BRPC cocultures stimulated and not stimulated for 1 h by *K. pneumoniae*. Values are expressed as the means ± SD of cytokine levels measured by three independent experiments performed in triplicate. Statistically significant differences, determined by one-way ANOVA and the Tukey posttest, are indicated (*, $P < 0.05$ versus control).

levels of VEGF than BREC monocultures, 1.6-fold higher than untreated BREC monocultures, which may act as a stabilizing factor for BREC. The presence of *K. pneumoniae* induced no increase in the VEGF secretion by BRPC. These data are in agreement with the results of our previous study showing that, in brain microvascular endothelial cells, PGE_2 action was associated with endothelial VEGF release (31). Moreover, in the untreated cocultures, the amount of VEGF was greater than the predicted sum of that produced in solo cultures. *K. pneumoniae* treatment of cocultures induced a 2.9-fold increase in comparison with the amounts in control untreated cocultures. Incubation of *K. pneumoniae*-treated BREC monocultures with 50 μM $AACOCF_3$, 2.5 μM BEL, or the COX-2-specific inhibitor NS-398 (5.0 μM) caused inhibition of *K. pneumoniae*-induced VEGF release by 70%, 67%, and 71%, respectively. Incubation of untreated cocultures with $AACOCF_3$, BEL, and NS-398 decreased VEGF release by about 28%, 25%, and 28%, respectively; in *K. pneumoniae*-treated cocultures the three inhibitors caused inhibition of VEGF release of 74%, 73%, and 75%, respectively. The effects of $AACOCF_3$, BEL, and NS-398 on VEGF release in untreated BRPC monocultures were decreases of about 23%, 19%, and 25%, respectively, and the inhibition was about 25%, 19%, and 36%, respectively, in *K. pneumoniae*-treated BRPC. These data indicate the involvement of PLA_2, AA production, and AA metabolization in eicosanoids in the production of PGE_2 and VEGF.

BREC-BRPC cocultures secrete IL-6 and IL-8 in response to stimulation by *K. pneumoniae* (Fig. 2). IL-6 and IL-8 levels were significantly elevated in infected cocultures in comparison to their levels in untreated cocultures.

***K. pneumoniae* cells adhere to BREC and BRPC, but no invasion occurs.** In Fig. 3, SEM images of BREC and BRPC grown on the membranes of the inserts, taken at 60 min postinfection with *K. pneumoniae*, show BREC with an elongated spindle phenotype and with numerous microvilli distributed on most of the cell surface (Fig. 3A). The images at higher magnification show the bacteria attached to the apical surface of the BREC, in contact with

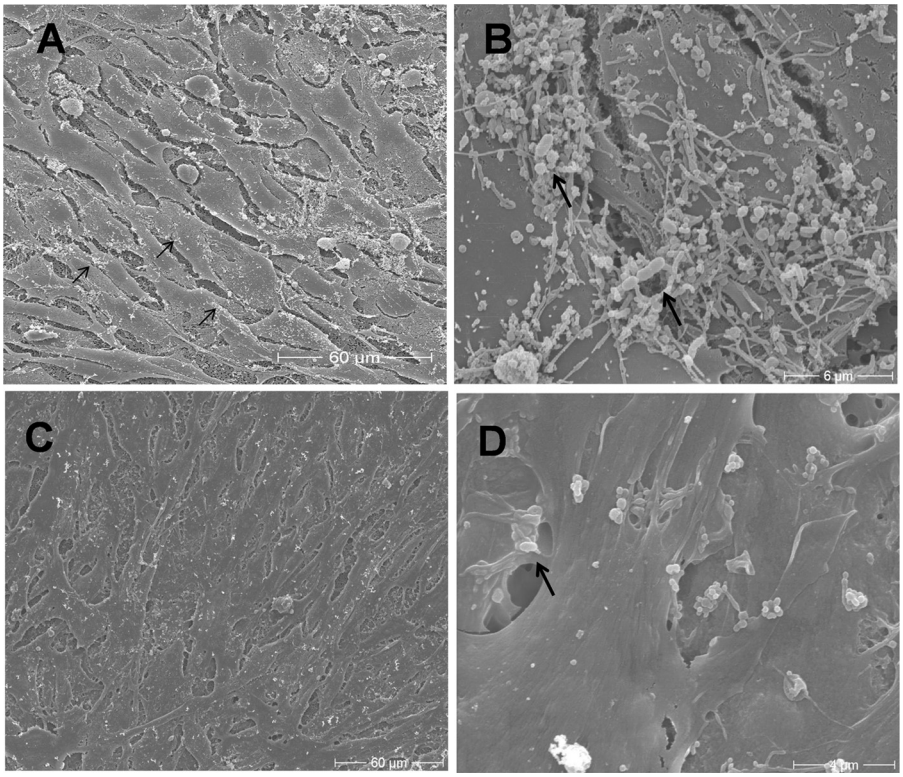

FIG 3 SEM of BREC and BRPC on Transwell filter at 60 min postinfection with *K. pneumoniae*. (A) BREC on Transwell filter at lower magnification show an elongated and spindled phenotype with numerous microvilli distributed over the surface and bacteria adhering in contact with them (black arrows). (B) BREC at higher magnification; typical short rod-shaped *K. pneumoniae* cells are visible on the surface, in contact with pseudopodia (black arrows). (C) BRPC exhibit a flattened shape with several branches. (D) Higher magnification shows the bacteria found on the cell surface (black arrow), in proximity to large pseudopodia.

pseudopodia (Fig. 3B). In Fig. 3C, SEM images of BRPC grown on the membrane of the inserts are shown. The cells are branched and flat, with short microvilli on the surface area. Few bacteria were found attached to the large pseudopodia of the BRPC surface without any sign of specific action on the membrane (Fig. 3D). Transmission electron micrographs of BREC and BRPC on Transwell filters at 60 min postinfection with *K. pneumoniae* are shown in Fig. 4. In the image in Fig. 4A, electron-dense bacteria appear to be in close contact with the endothelial cell membrane and no intracellular bacteria are visible. Figure 4B shows the adhesion of *K. pneumoniae* to the surface of BREC, and no internalized bacteria are visible. Figure 4C shows BRPC with evident micropinocytotic transport. Numerous bacteria, rounded or elongated in shape, are present on the outside and in the space between the two pericytes, but in this case also, no intracellular bacteria are found. In Fig. 4D, a tight junction-like apparatus is visible between two cells, but no evidence of membrane fusion is observed. Micropinocytotic transport and large lipid granules, lysosome, and small protein-containing vacuoles are visible in the cytoplasm in Fig. 4D. These data confirmed the results obtained in adhesion and invasion assays (data not shown). Experiments were also performed with human retinal cells. TEM of HREC and HRPC grown on the membrane of the inserts at 60 min postinfection with *K. pneumoniae* did not show intracellular bacteria (data not shown).

***K. pneumoniae* increased $cPLA_2$, $iPLA_2$, and COX1/2expression.** The Western blot analysis in Fig. 5 showed no changes in the protein levels of $cPLA_2$ in control and infected BREC and BRPC. The phosphorylated form of $cPLA_2$ increased significantly in *K. pneumoniae*-infected BREC, by 5.6-fold compared to the level in the control BREC. Thus, the increase of $cPLA_2$ phosphorylation ($p\text{-}cPLA_2/cPLA_2$ ratios were 0.31 to 1.43 for infected BREC) may support an increase in $cPLA_2$ activity. Incubation of BRPC with *K. pneumoniae* produced no phosphorylation in $cPLA_2$ in comparison with that in control BRPC, confirming the results presented in Table 2, in which enzyme activity in BRPC was not activated by the infection. Moreover, $iPLA_2$ expression was increased about 2.9-fold in BREC infected with *K. pneumoniae*. There was no change in $iPLA_2$ expression after treatment of BRPC with bacteria. These results confirm our findings described above (Table 2) that implicate both endothelial $cPLA_2$ and $iPLA_2$ in the increased total PLA_2 activity seen in response to *K. pneumoniae* treatment. In a set of preliminary experiments, we observed that the presence of $sPLA_2$ in BREC and BRPC was barely detectable, and we also found that $sPLA_2$ (IIA) was not upregulated by *K. pneumoniae* treatment (data not shown). Because COX-1 and COX-2 govern the rate-limiting step in the conversion of AA to its downstream prostanoid effectors, we evaluated COX-1 and COX-2 expression in BREC and BRPC (Fig. 5C and D). No change was found in COX-1 protein expression in the two cellular types after bacterial infection. BREC expressed COX-2 total protein at levels significantly higher (about 2.8-fold) than the uninfected control, whereas the protein levels in BRPC after *K. pneumoniae* infection remained unchanged compared to the levels in uninfected cells.

$cPLA_2$ and $iPLA_2$ negatively regulate BRPC survival, and their blockade protects the barrier integrity. To verify whether the prevention of PLA_2 activation can reduce the damage to the

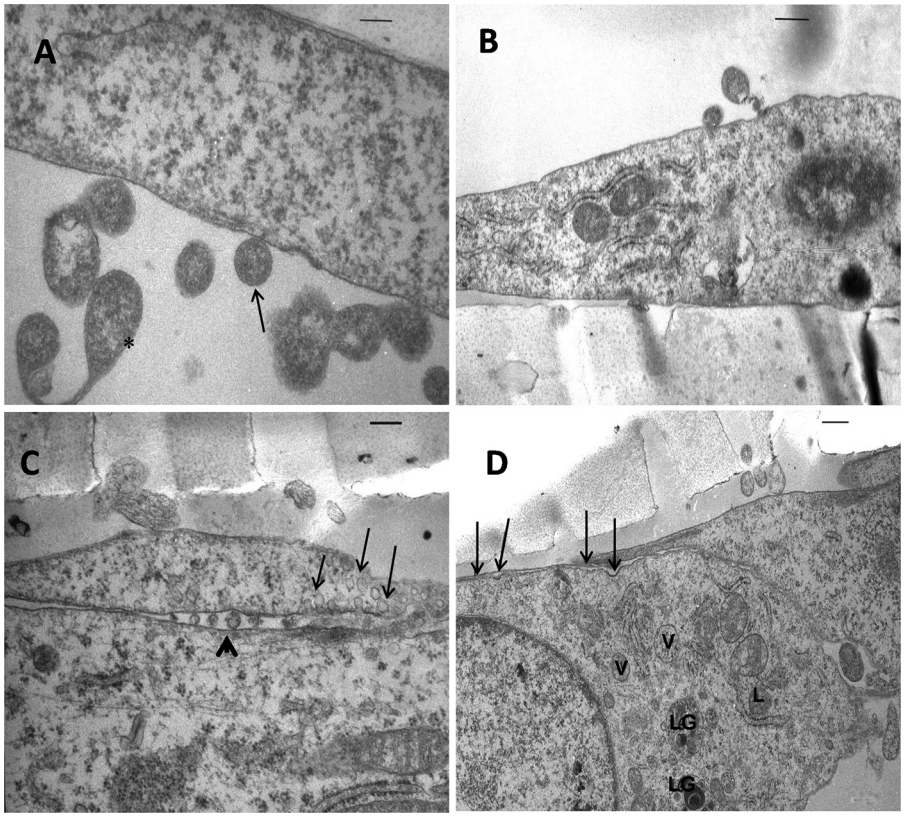

FIG 4 Transmission electron micrographs of BREC and BRPC on Transwell filter at 60 min postinfection with *K. pneumoniae*. (A) BREC infected by *K. pneumoniae*. Electron-dense (dark black) bacteria appear to be in close contact with the endothelial cell membrane (black arrow). A bacterium that is dividing is visible (*). Bar = 120 nm. (B) Adhesion of *K. pneumoniae* to the BREC surface; no intracellular bacteria are visible. Bar = 0.399 μm. (C) BRPC showing increased micropinocytotic transport (black arrows). Numerous bacteria, rounded or elongated in shape (arrowhead), are present on the outside and in the space between two pericytes. Bar = 0.198 μm. (D) Tight junction-like apparatus between two BRPC and micropinocytotic transport (thin arrows). In the BRPC cytoplasm, large lipid granules (LG), lysosome (L), and small protein-containing vacuoles (V) are visible. Bar = 0.4 μm.

BRB after *K. pneumoniae* infection, we used small interfering RNA-mediated silencing of endothelial PLA_2 expression (Fig. 6). In our experimental model, BREC were transfected with an empty vector (control BREC), nontargeting siRNA (nt-siRNA-BREC), $cPLA_2$ siRNA ($cPLA_2$ siRNA-BREC), or $iPLA_2$ siRNA ($iPLA_2$ siRNA-BREC). After transfection, BREC were cultured until confluence on the Transwell insert in which BRPC were grown on the lower side of the membrane (Fig. 6A). After reaching confluence, the cocultures were infected or not with *K. pneumoniae* for 60 min. The numbers of control BREC, nt-siRNA-BREC, $cPLA_2$ siRNA-BREC, or $iPLA_2$ siRNA-BREC grown in coculture with BRPC were not changed after infection with *K. pneumoniae* (Fig. 6B). In contrast, the number of BRPC grown in coculture with nt-BREC was significantly reduced, by about 60%, after *K. pneumoniae* infection compared to the number in uninfected BRPC grown under the same conditions (Fig. 6C). Surprisingly, when BRPC were cocultured with $cPLA_2$ siRNA-BREC or $iPLA_2$ siRNA-BREC, after incubation for 60 min with *K. pneumoniae*, the numbers of BRPC were about 2.1-fold and 1.9-fold higher than the numbers in infected BRPC cocultured with nt-siRNA-BREC.

These results were confirmed by TEER and permeability measurements. In nt-siRNA–BREC-BRPC cocultures infected with *K. pneumoniae*, the TEER values were already decreased after 30 min of treatment (39% reduction), and they were decreased by 48% and 76% after 60 and 120 min, respectively (Fig. 6E). When $cPLA_2$ siRNA-BREC or $iPLA_2$ siRNA-BREC were cocultured with BRPC, the TEER values increased by 1.6- and 1.3-fold after 60 min of *K. pneumoniae* infection and by 3.0- and 2.7-fold after 120 min, respectively, in comparison with the values in infected nt-siRNA–BREC-BRPC. Moreover, in cPLA2 siRNA-BREC, permeability to sodium fluorescein increased by about 3.8-fold in comparison with the permeability of nt-siRNA–BREC-BRPC after 60 min of *K. pneumoniae* infection (Fig. 6F), and when $cPLA_2$ siRNA-BREC or $iPLA_2$ siRNA-BREC were cocultured with BRPC in the presence of *K. pneumoniae*, permeability decreased, respectively, by about 2.1- and 1.9-fold after 60 min and by 2.0- and 1.7-fold after 120 min of bacterial infection in comparison with the sodium fluorescein permeability of infected nt-siRNA–BREC-BRPC.

These results demonstrated once more that enhanced PLA_2 enzyme activities are an absolute intermediate requirement for the attack on the BRB by *K. pneumoniae* and that the prevention of pericyte loss and monolayer permeability can be attributed to blockade of PLA_2s.

Western immunoblot assays using lysates obtained from three separate preparations of BREC revealed the specificity of the siRNAs used. The basal protein expression levels of both $cPLA_2$ and $iPLA_2$ were strongly attenuated in transfected BRECs, by approximately 90% for $cPLA_2$ and 85% for $iPLA_2$ (Fig. 6D, lanes 3 and 4, respectively), compared with the levels in cells transfected with either an empty vector (Fig. 6D, control BREC, lane 1) or

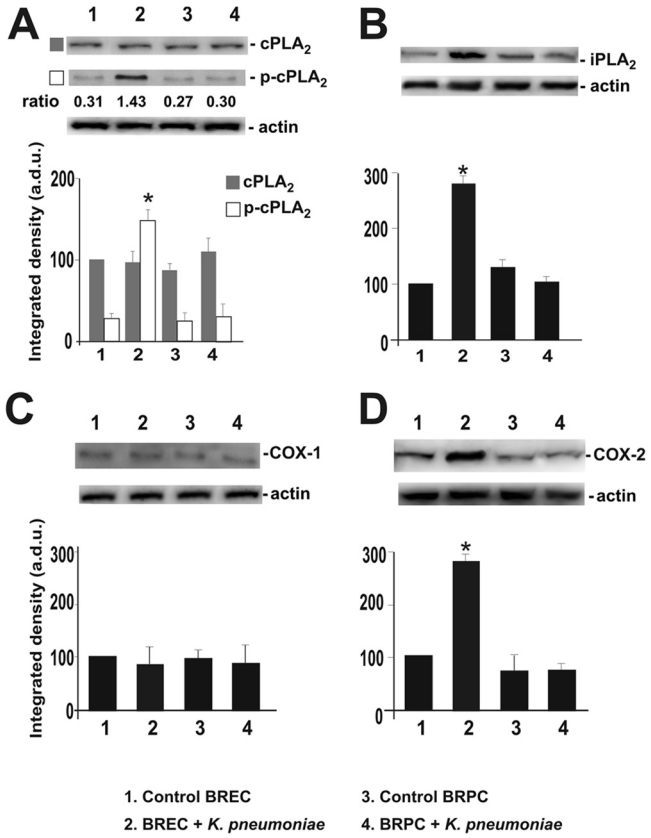

FIG 5 Western blot analyses of $cPLA_2$ and phospho-$cPLA_2$ (A), $iPLA_2$ (B), COX-1 (C), and COX-2 (D) in BREC and BRPC stimulated or not with *K. pneumoniae*. The values, expressed as arbitrary densitometric units (a.d.u.), were obtained by reading the blots using the Image J program and are the means ± SD from three independent experiments ($n = 3$) performed in triplicate. Statistically significant differences, determined by one-way ANOVA and the Tukey posttest, are indicated (*, $P < 0.05$).

nontargeting siRNA-BREC (Fig. 6D, lane 2). Similar TEER measurements were performed in HREC-HRPC cocultures that used the experimental model depicted in Fig. 6A. In nt-siRNA–HREC-HRPC cocultures, the TEER values decreased by 2.1- and 6.2-fold, respectively, after 60 and 120 min of *K. pneumoniae* infection (Fig. 6G), and when $cPLA_2$ siRNA-HREC or $iPLA_2$ siRNA-HREC were cocultured with HRPC, the TEER values increased, respectively, by 1.7- and 1.3-fold after 60 min and by 4.2- and 3.0-fold after 120 min of *K. pneumoniae* infection in comparison with the values in infected nt-siRNA–HREC-HRPC. The percent cell counts of human cells in cocultures, under all experimental conditions (Fig. 6A) and in the presence or absence of *K. pneumoniae*, were very similar to those obtained in BREC-BRPC cocultures (data not shown).

DISCUSSION

Endogenous *Klebsiella* endophthalmitis is an uncommon condition with severe complications. An early diagnosis and aggressive antibiotic therapy can improve the final course, but the visual outcome still remains poor (37). The entry of circulating bacteria into the retina requires crossing the BRB, composed of retinal microvascular EC which have a dynamic interaction with other neighboring cells, these being BRPC, astrocytes, and Müller cells (21, 22). Despite the fact that the BRPC are morphologically situated closest to BREC, with which they share a basement membrane, they have been the subject of very few studies for testing the molecular mechanisms of bacterial invasion.

In the present study, using an *in vitro* model of *K. pneumoniae* infection on BREC-BRPC in coculture, we tested the hypothesis that *K. pneumoniae* induces an inflammatory response in these blood retinal barrier cells. There is only a limited body of evidence that pathogenic bacteria elicit inflammatory responses at this specific retinal cell layer. In experimental *in vivo* animal studies, it has been demonstrated that endophthalmitis induced by *Bacillus cereus* and *Staphylococcus epidermidis* caused increased production of proinflammatory cytokines that may contribute to barrier breakdown (38, 39). An *in vitro* study demonstrated a proinflammatory effect of *K. pneumoniae* on retinal pigmented epithelial cells, with an increase of IL-6 and monocyte chemotactic protein-1 levels (18), and an *in vivo* study reported the overexpression of IL-17 in the pulmonary compartment of C57BL/6 mice after challenge with *Klebsiella pneumoniae* (40).

K. pneumoniae has become an important pathogen in recent years, causing pyogenic liver abscesses and other soft tissue abscesses. From these tissue abscesses, *K. pneumoniae* can spread to the eye or meninges, causing metastatic endophthalmitis, meningitis, or both (14). The BRB, because the intercellular spaces between retinal endothelial cells are sealed by elaborate tight junction cells, is a defense against hematogenous pathogenic bacteria.

The *in vitro* BRB model used in our experiments showed high TEER and low permeability, indicators of barrier integrity that we consider very useful for studying the cell response to bacterial infection of the BRB. In BREC-BRPC cocultures, *K. pneumoniae* infection produces significant reduction of TEER and increase in permeability. Moreover, we demonstrated that $cPLA_2$ and $iPLA_2$ activities, as well as PGE_2 and VEGF levels, were increased in BREC in cocultures after *K. pneumoniae* incubation. Interestingly, the significant decrease in BREC phospholipase activity in the presence of BEL suggests a major contribution of endothelial $iPLA_2$ in mediating AA release after *K. pneumoniae* infection. These results were confirmed by the incremental expression of $cPLA_2$, $iPLA_2$, and COX1/2, as well as the increased $cPLA_2$ phosphorylation, in BREC after *K. pneumoniae* coculture incubation. These orchestrated events are expected to increase the levels of PGs, because the activation of $cPLA_2$ elicits arachidonic acid (AA), a substrate for PG production by COX enzymes from membrane phospholipids. Inhibition of PLA_2, using either BEL, an $iPLA_2$-specific compound, or $AACOCF_3$, a $cPLA_2$/$iPLA_2$ selective compound, reduced the *K. pneumoniae*-induced elevation of PGE_2. Moreover, the presence of PLA_2 inhibitors and of NS-392, a COX-specific inhibitor, reduced VEGF release in BREC and BRPC, indicating that PGs could exert a proangiogenic influence by inducing VEGF production upon binding to target genes in endothelial cells. In addition, BRPC release physiologically higher levels of VEGF than do BREC, which may act as a stabilizing factor for BREC.

These data are in agreement with the results of previous studies showing that PGE_2 stimulates VEGF expression in rat Müller cells (41), and in microvascular endothelial cells, PGE_2 activity was associated with endothelial VEGF release (42). In agreement with this, in monkey choroid-retinal endothelial cells, VEGF release results from hypoxia-induced activation of $cPLA_2$ (43), and in retinal endothelial cells, arachidonic acid, converted by the cyclo-

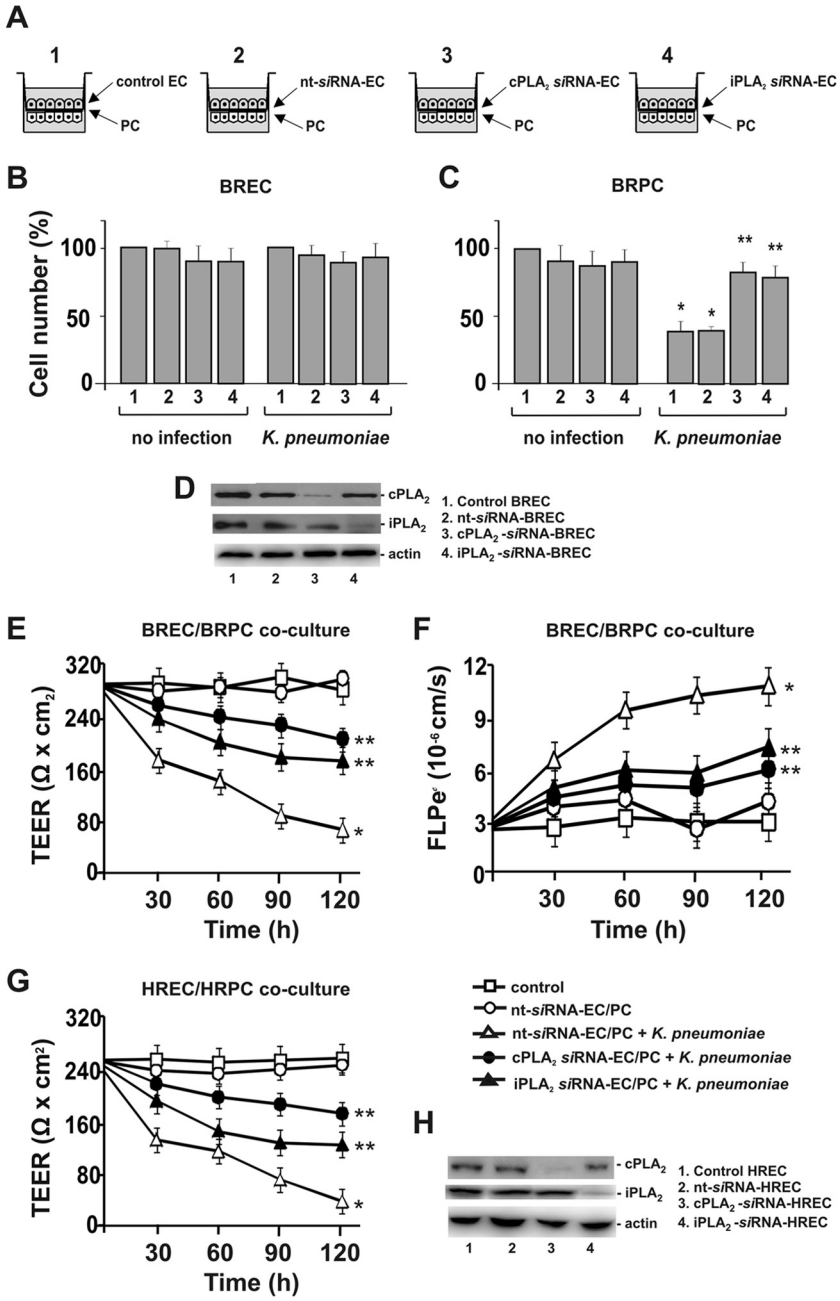

FIG 6 Effects of *K. pneumoniae* infection on proliferation of BREC and BRPC in coculture and on TEER and permeability to sodium fluorescein. (A) The experimental model is depicted. BREC were transfected with empty vector (control EC), nontargeting siRNA (nt-siRNA-EC), $cPLA_2$ siRNA ($cPLA_2$ siRNA-EC), or $iPLA_2$ siRNA ($iPLA_2$ siRNA-EC). After transfection, BREC were cultured until confluence on the Transwell insert (40,000 cells cm^2) in which BRPC were grown on the lower side of the membrane. Cocultures were incubated or not with *K. pneumoniae* for 1 h. (B) For the proliferation study, after incubation for 1 h with or without *K. pneumoniae*, cells from inserts (0.4-μm pore size) were trypsinized separately. The numbers of live control BREC, nt-siRNA-BREC, $cPLA_2$ siRNA-BREC, and $iPLA_2$ siRNA-BREC grown in coculture with BRPC were determined by counting viable cells using trypan blue exclusion assay. (C) The numbers of live BRPC grown in the cocultures were determined with the same procedure described for panel B. (D) Parallel cultures were collected and subjected to Western blot analysis to confirm the reduction of $cPLA_2$ and $iPLA_2$ protein levels in siRNA-treated BREC. Representative gel runs are shown. (E and F) Transendothelial electrical resistance (TEER) (E) and permeability to sodium fluorescein (F) of BREC-BRPC, nt-siRNA–BREC-BRPC, $cPLA_2$ siRNA–BREC-BRPC, or $iPLA_2$ siRNA–BREC-BRPC cocultures on Transwell inserts in the presence or absence of *K. pneumoniae* were determined as described in Materials and Methods. (G) TEER measurements were determined for HREC-HRPC, nt-siRNA–HREC-HRPC, $cPLA_2$ siRNA–HREC-HRPC, or $iPLA_2$ siRNA–HREC-HRPC cocultures on Transwell inserts using the experimental model depicted in panel A and in the presence or absence of *K. pneumonia*. (H) Western blot analysis confirmed the reduction of $cPLA_2$ and $iPLA_2$ protein levels in siRNA-treated HREC. Values are expressed as the means ± SD from three independent experiments performed in triplicate. The same time points were compared among different conditions when performing the statistical analysis. Statistically significant differences, determined by one-way ANOVA and the Tukey posttest, are indicated (*, $P < 0.05$ versus control; **, $P < 0.05$ versus nt-siRNA–BREC-BRPC in the presence of *K. pneumoniae*).

oxygenase enzymes in prostaglandins, induces VEGF production (44). It has been demonstrated that endothelial cells participate in modulating the inflammatory response through cytokine signaling (28, 45). BREC-BRPC cocultures, after exposure to *K. pneumoniae*, released elevated levels of IL-6 and IL-8. Conceivably, by increasing the interleukin levels, endothelial cells potentiate the inflammatory response by activating circulating intravascular cells. Proinflammatory cytokines could modify the protein constituents of tight junctions. A recent study demonstrated that treatment with IL-6 reduced occludin expression in cerebral microvessels from yearling and adult sheep, highlighting the idea that cytokines play an important role in blood brain barrier dysfunction (46). We speculate that IL-6 and IL-8, which were released in the coculture medium after *K. pneumoniae* infection, could contribute to the loss of retinal barrier function.

It was interesting to see that *K. pneumoniae* infection resulted in a reduction of pericytes and, as expected, a decrease of TEER values and an increase of permeability in our BRB model. Following *K. pneumoniae* infection of cocultures in which BREC were transfected with $cPLA_2$ or $iPLA_2$ siRNA, the pericyte numbers were very similar to the numbers of BRPC grown in contact with nontransfected BREC in the absence of infection, and the values of TEER and permeability to sodium fluorescein were restored. These results, confirmed by those obtained from similar experiments on human endothelial cells and human pericytes in coculture, demonstrated the important role played by PLA_2s in maintaining barrier properties. We speculated that VEGF released by endothelial cells could bind to VEGF receptors on the membrane of adjacent pericytes and result in their leakage, acting as a negative regulator and, thus, increasing BRB permeability. The negative role of VEGF in pericyte function has recently been shown in the $C_3$10T1/2 pericyte line, revealing a dichotomous role for VEGF, which is already known as a promoter of endothelial cells (47). Moreover, it has been demonstrated that the systemic delivery of VEGF ablates pericytes from the mature retinal vasculature through the VEGFR1-mediated signaling pathway, leading to increased vascular leakage, and the blockade of VEGFR-1 significantly restores BRPC saturation in mature vessels (29), suggesting that retinal pericytes play a crucial role in BRB integrity under healthy conditions.

Only a few bacteria are able to enter the cells. Pathogenic bacteria have developed individual strategies which allow them to adhere to and cross the brain endothelium. In a previous study, we demonstrated that *E. coli* cells interact with endothelial receptors and enter the brain through an endothelial transcellular mechanism, causing the wearing down of the blood-brain barrier and triggering an inflammatory response mediated by PGs and VEGF release (31). The results obtained in our study on *K. pneumoniae* infection indicate that similar inflammatory responses can also occur after a bacterial infection not mediated by a transcellular endothelial crossing.

The TEM and SEM images showed that *K. pneumoniae* adhered to but did not enter BREC and BRPC, as well as HREC and HRPC. Different bacterial phenotypes exist, with specific sets of virulence factors expressed by the organism that explain different clinical features of bacterial infection with *K. pneumoniae* (48). The limited invasion of strain 43816 in retinal microvascular endothelial cells demonstrates that host cell invasion is not necessarily a prerequisite for inflammation and pathogenicity. Enterohemorrhagic *E. coli* (EHEC) strains, which are associated with severe disease, attach to the epithelial cell surface but do not invade (49). Similarly, enteropathogenic *E. coli* (EPEC), the causative agent of severe diarrhea that can lead to mortality in humans and animals, are not invasive (50). In testing clinical isolates, it has been observed that some *K. pneumoniae* strains possess higher invasive potential, probably due to specific genes, in addition to a great difference in invasion depending on the host cell type (51).

Our results showed the proinflammatory effect of *K. pneumoniae* on retinal microvascular endothelial cells and the important defensive role played by the pericytes during a bacterial attack. Pericytes could be considered the cells which oversee the defense of the retinal barrier, and their survival enables the maintenance of a stronghold which opposes bacterial infection.

The leakage of a certain number of pericytes is one of the mechanisms that might be strongly correlated to the loss of retinal barrier function, and it appears to compromise the resistance of endothelial cells to the bacterial infection. Moreover, major questions remain unanswered. Why, for instance, is a much lower number of pericytes than of retinal microvessels enough to stabilize the vasculature in other parts of the body, whereas a partial decrease in the pericyte coverage of retinal microvessels results in the loss of BRB functions? Why and how do pericytes fall off the retinal microvessels and how does this impair endothelial cell function and microvessel stability? Can we prevent or limit these mechanisms once they are elucidated? Attempting to answer these questions stimulates us to work on pericyte biology and pathology, as the field may provide physicians and patients with new ways to fight blinding diseases.

A proper pharmacological action on the enzymes involved in *K. pneumoniae* infection, the mediators of the BRPC detachment from microvessels on which *K. pneumoniae* develops its invasive strategy to have free access to the retina, would be to slow down BRPC loss, thus protecting the anatomical integrity of the microvessels. The combination of an antibiotic therapy with a drug able to block this action on the BRPC could represent a novel strategy to treat bacterial endogenous endophthalmitis more successfully. A better understanding of the mechanisms by which *K. pneumoniae* alters the communication between microvascular retinal endothelial cells and pericytes may provide exciting new insights into the potential for clinical intervention.

ACKNOWLEDGMENTS

With pleasure we express our gratitude to Francesco Avola for his skilled assistance; he has greatly facilitated our work, contributing to the achievement of many of the results presented here.

This work was supported by National grant PRIN 2009-BM7LJC.

REFERENCES

1. **Coburn PS, Wiskur BJ, Christy E, Callegan MC.** 2012. The diabetic ocular environment facilitates the development of endogenous bacterial endophthalmitis. Invest. Ophthalmol. Vis. Sci. **53:**7426–7431. http://dx.doi.org/10.1167/iovs.12-10661.
2. **Cabana-Carcasi ML, Becerra-Mosquera V, González-Tabarés L, Novoa-García D.** 2012. Endogenous endophthalmitis as a complication of sepsis related to a tunnelled haemodialysis catheter. Nefrologia **32:**255–256.
3. **Cornut PL, Chiquet C.** 2011. Endogenous bacterial endophthalmitis. J. Fr. Ophtalmol. **34:**51–57. http://dx.doi.org/10.1016/j.jfo.2010.08.007.
4. **Yodprom R, Pathanapitoon K, Kunavisarut P, Ausayakhun S, Wattananikorn S, Rothova A.** 2007. Endogenous endophthalmitis due to *Salmonella choleraesuis* in an HIV-positive patient. Ocul. Immunol. Inflamm. **15:**135–138. http://dx.doi.org/10.1080/09273940701244228.
5. **Maruno T, Ooiwa Y, Takahashi K, Kodama Y, Takakura S, Ichiyama S, Chiba T.** 2013. A liver abscess deprived a healthy adult of eyesight: endog-

enous endophthalmitis associated with a pyogenic liver abscess caused by serotype K1 *Klebsiella pneumonia*. Intern. Med. **52:**919–922. http://dx.doi.org/10.2169/internalmedicine.52.9076.
6. **Basu S, Kumar A, Kapoor K, Bagri NK, Chandra A.** 2013. Neonatal endogenous endophthalmitis: a report of six cases. Pediatrics **131:**e1292–7. http://dx.doi.org/10.1542/peds.2011-3391.
7. **Durand ML.** 2013. Endophthalmitis. Clin. Microbiol. Infect. **19:**227–234. http://dx.doi.org/10.1111/1469-0691.12118.
8. **Ang M, Jap A, Chee SP.** 2011. Prognostic factors and outcomes in endogenous *Klebsiella pneumoniae* endophthalmitis. Am. J. Ophthalmol. **151:**338–344. http://dx.doi.org/10.1016/j.ajo.2010.08.036.
9. **Chung KS, Kim YK, Song YG, Kim CO, Han SH, Chin BS, Gu NS, Jeong SJ, Baek JH, Choi JY, Kim HY, Kim JM.** 2011. Clinical review of endogenous endophthalmitis in Korea: a 14-year review of culture positive cases of two large hospitals. Yonsei Med. J. **52:**630–634. http://dx.doi.org/10.3349/ymj.2011.52.4.630.
10. **Pomakova DK, Hsiao CB, Beanan JM, Olson R, MacDonald U, Keynan Y, Russo TA.** 2012. Clinical and phenotypic differences between classic and hypervirulent *Klebsiella pneumonia*: an emerging and under-recognized pathogenic variant. Eur. J. Clin. Microbiol. Infect. Dis. **31:**981–989. http://dx.doi.org/10.1007/s10096-011-1396-6.
11. **Cortés G, Borrell N, de Astorza B, Gómez C, Sauleda J, Albertí S.** 2002. Molecular analysis of the contribution of the capsular polysaccharide and the lipopolysaccharide O side chain to the virulence of *Klebsiella pneumoniae* in a murine model of pneumonia. Infect. Immun. **70:**2583–2590. http://dx.doi.org/10.1128/IAI.70.5.2583-2590.2002.
12. **Frazee BW, Hansen S, Lambert L.** 2009. Invasive infection with hypermucoviscous *Klebsiella pneumoniae*: multiple cases presenting to a single emergency department in the United States. Ann. Emerg. Med. **53:**639–642. http://dx.doi.org/10.1016/j.annemergmed.2008.11.007.
13. **Pastagia M, Arumugam V.** 2008. *Klebsiella pneumoniae* liver abscesses in a public hospital in Queens, New York. Travel Med. Infect. Dis. **6:**228–233. http://dx.doi.org/10.1016/j.tmaid.2008.02.005.
14. **Sobirk SK, Struve C, Jacobsson SG.** 2010. Primary *Klebsiella pneumoniae* liver abscess with metastatic spread to lung and eye: a North-European case report of an emerging syndrome. Open Microbiol. J. **4:**5–7. http://dx.doi.org/10.2174/1874285801004010005.
15. **Turton JF, Englender H, Gabriel SN, Turton SE, Kaufmann ME, Pitt TL.** 2007. Genetically similar isolates of *Klebsiella pneumoniae* serotype K1 causing liver abscesses in three continents. J. Med. Microbiol. **56:**593–597. http://dx.doi.org/10.1099/jmm.0.46964-0.
16. **Karama EM, Willermain F, Janssens X, Claus M, Van den Wijngaert S, Wang JT, Verougstraete C, Caspers L.** 2008. Endogenous endophthalmitis complicating *Klebsiella pneumoniae* liver abscess in Europe: case report. Int. Ophthalmol. **28:**111–113. http://dx.doi.org/10.1007/s10792-007-9111-4.
17. **Fang CT, Chuang YP, Shun CT, Chang SC, Wang JT.** 2004. A novel virulence gene in *Klebsiella pneumoniae* strains causing primary liver abscess and septic metastatic complications. J. Exp. Med. **199:**697–705. http://dx.doi.org/10.1084/jem.20030857.
18. **Pollreisz A, Rafferty B, Kozarov E, Lalla E.** 2012. *Klebsiella pneumoniae* induces an inflammatory response in human retinal-pigmented epithelial cells. Biochem. Biophys. Res. Commun. **418:**33–37. http://dx.doi.org/10.1016/j.bbrc.2011.12.102.
19. **Cunha-Vaz J, Bernardes R, Lobo C.** 2011. Blood-retinal barrier. Eur. J. Ophthalmol. **21**(Suppl 6):S3–S9. http://dx.doi.org/10.5301/EJO.2010.6049.
20. **Klaassen I, Van Noorden CJ, Schlingemann RO.** 2013. Molecular basis of the inner blood-retinal barrier and its breakdown in diabetic macular edema and other pathological conditions. Prog. Retin. Eye Res. **34:**19–48. http://dx.doi.org/10.1016/j.preteyeres.2013.02.001.
21. **Runkle EA, Antonetti DA.** 2011. The blood-retinal barrier: structure and functional significance, p 133–148. *In* Nag S (ed), Methods in molecular biology, vol 686:the blood-brain and other neural barriers—reviews and protocols. Humana Press, New York, NY.
22. **Winkler EA, Bell RD, Zlokovic BV.** 2011. Central nervous system pericytes in health and disease. Nat. Neurosci. **14:**398–1405.
23. **Kim JH, Kim JH, Yu YS, Kim DH, Kim KW.** 2009. Recruitment of pericytes and astrocytes is closely related to the formation of tight junction in developing retinal vessels. J. Neurosci. Res. **87:**653–659. http://dx.doi.org/10.1002/jnr.21884.
24. **Nag S.** 2011. The blood-brain and other neural barriers—reviews and protocols. Methods in Molecular Biology, vol 686. Humana Press, New York, NY.
25. **Motiejunaite R, Kazlauskas A.** 2008. Pericytes and ocular diseases. Exp. Eye Res. **86:**171–177. http://dx.doi.org/10.1016/j.exer.2007.10.013.
26. **Alberghina M.** 2010. Phospholipase A(2): new lessons from endothelial cells. Microvasc. Res. **80:**280–285. http://dx.doi.org/10.1016/j.mvr.2010.03.013.
27. **de Toledo A, Nagata E, Yoshida Y, Oho T.** 2012. Streptococcus oralis coaggregation receptor polysaccharides induce inflammatory responses in human aortic endothelial cells. Mol. Oral Microbiol. **27:**295–307. http://dx.doi.org/10.1111/j.2041-1014.2012.00646.x.
28. **Ferrero MC, Bregante J, Delpino MV, Barrionuevo P, Fossati CA, Giambartolomei GH, Baldi PC.** 2011. Proinflammatory response of human endothelial cells to Brucella infection. Microbes Infect. **13:**852–861. http://dx.doi.org/10.1016/j.micinf.2011.04.010.
29. **Cao R, Xue Y, Hedlund EM, Zhong Z, Tritsaris K, Tondelli B, Lucchini F, Zhu Z, Dissing S, Cao Y.** 2010. VEGFR1-mediated pericyte ablation links VEGF and PIGF to cancer-associated retinopathy. Proc. Natl. Acad. Sci. U. S. A. **107:**856–861. http://dx.doi.org/10.1073/pnas.0911661107.
30. **Salmeri M, Motta C, Mastrojeni S, Amodeo A, Anfuso CD, Giurdanella G, Morello A, Alberghina M, Toscano MA, Lupo G.** 2012. Involvement of PKCα-MAPK/ERK-phospholipase A(2) pathway in the *Escherichia coli* invasion of brain microvascular endothelial cells. Neurosci. Lett. **511:**33–37. http://dx.doi.org/10.1016/j.neulet.2012.01.031.
31. **Salmeri M, Motta C, Anfuso CD, Amodeo A, Scalia M, Toscano MA, Alberghina M, Lupo G.** 2013. VEGF receptor-1 involvement in pericyte loss induced by *Escherichia coli in* an *in vitro* model of blood brain barrier. Cell. Microbiol. **15:**1367–1384. http://dx.doi.org/10.1111/cmi.12121.
32. **Giurdanella G, Motta C, Muriana S, Arena V, Anfuso CD, Lupo G, Alberghina M.** 2011. Cytosolic and calcium-independent phospholipase A_2 mediate glioma-enhanced proangiogenic activity of brain endothelial cells. Microvasc. Res. **81:**1–17. http://dx.doi.org/10.1016/j.mvr.2010.11.005.
33. **Lupo G, Anfuso CD, Ragusa N, Strosznajder RP, Walski M, Alberghina M.** 2001. t-Butyl hydroperoxide and oxidized low density lipoprotein enhance phospholipid hydrolysis in lipopolysaccharide-stimulated retinal pericytes. Biochim. Biophys. Acta **1531:**143–155. http://dx.doi.org/10.1016/S1388-1981(01)00102-0.
34. **Lupo G, Assero G, Anfuso CD, Nicotra A, Palumbo M, Cannavò G, Renis M, Ragusa N, Alberghina M.** 2002. Cytosolic phospholipase A_2 mediates arachidonoyl phospholipid hydrolysis in immortalized rat brain endothelial cells stimulated by oxidized LDL. Biochim. Biophys. Acta **1585:**19–29. http://dx.doi.org/10.1016/S1388-1981(02)00303-7.
35. **Anfuso CD, Lupo G, Romeo L, Giurdanella G, Motta C, Pascale A, Tirolo C, Marchetti B, Alberghina M.** 2007. Endothelial cell-pericyte cocultures induce PLA2 protein expression through activation of PKCalpha and the MAPK/ERK cascade. J. Lipid Res. **48:**782–793. http://dx.doi.org/10.1194/jlr.M600489-JLR200.
36. **Zhu L, Maruvada R, Sapirstein A, Malik KU, Peters-Golden M, Kim KS.** 2010. Arachidonic acid metabolism regulates Escherichia coli penetration of the blood-brain barrier. Infect. Immun. **78:**4302–4310. http://dx.doi.org/10.1128/IAI.00624-10.
37. **Batres Iglesias AP, Pérez Cabeza MI, Del Río Pardo MJ, Castaño M.** 2011. Endogenous endophthalmitis as a first clinical manifestation of Klebsiella sepsis. The importance of an early diagnosis. Arch. Soc. Esp. Oftalmol. **86:**412–414. http://dx.doi.org/10.1016/j.oftal.2011.06.016.
38. **Moyer AL, Ramadan RT, Novosad BD, Astley R, Callegan MC.** 2009. Bacillus cereus-induced permeability of the blood-ocular barrier during experimental endophthalmitis. Invest. Ophthalmol. Vis. Sci. **50:**3783–3793. http://dx.doi.org/10.1167/iovs.08-3051.
39. **Petropoulos IK, Vantzou CV, Lamari FN, Karamanos NK, Anastassiou ED, Pharmakakis NM.** 2006. Expression of TNF-alpha, IL-1beta, and IFN-gamma in Staphylococcus epidermidis slime-positive experimental endophthalmitis is closely related to clinical inflammatory scores. Graefes Arch. Clin. Exp. Ophthalmol. **244:**1322–1328. http://dx.doi.org/10.1007/s00417-006-0261-2.
40. **Ye P, Garvey PB, Zhang P, Nelson S, Bagby G, Summer WR, Schwarzenberger P, Shellito JE, Kolls JK.** 2001. Interleukin-17 and lung host defense against Klebsiella pneumoniae infection. Am. J. Respir. Cell Mol. Biol. **25:**335–340. http://dx.doi.org/10.1165/ajrcmb.25.3.4424.
41. **Cheng T, Cao W, Wen R, Steinberg RH, LaVail MM.** 1998. Prostaglandin E_2 induces vascular endothelial growth factor and basic fibroblast

growth factor mRNA expression in cultured rat Muller Cells. Invest. Ophthalmol. Vis. Sci. **39:**581–591.
42. **Pai R, Szabo IL, Soreghan BA, Atay S, Kawanaka H, Tarnawski AS.** 2001. PGE(2) stimulates VEGF expression in endothelial cells via ERK2/JNK1 signaling pathways. Biochem. Biophys. Res. Commun. **286:**923–928. http://dx.doi.org/10.1006/bbrc.2001.5494.
43. **Ottino P, Finley J, Rojo E, Ottlecz A, Lambrou GN, Bazan HE, Bazan NG.** 2004. Hypoxia activates matrix metalloproteinase expression and the VEGF system in monkey choroid-retinal endothelial cells: involvement of cytosolic phospholipase A_2 activity. Mol. Vis. **10:**341–350. http://www.molvis.org/molvis/v10/a43/.
44. **Barnett JM, McCollum GW, Penn JS.** 2010. Role of cytosolic phospholipase A(2) in retinal neovascularization. Invest. Ophthalmol. Vis. Sci. **51:**1136–1142. http://dx.doi.org/10.1167/iovs.09-3691.
45. **Soult MC, Lonergan NE, Shah B, Kim W-K, Britt LD, Sullivan CJ.** 2013. Outer membrane vesicles from pathogenic bacteria initiate an inflammatory response in human endothelial cells. J. Surg. Res. **184:**458–466. http://dx.doi.org/10.1016/j.jss.2013.05.035.
46. **Cohen SS, Min M, Cummings EE, Chen X, Sadowska GB, Sharma S, Stonestreet BS.** 2013. Effects of interleukin-6 on the expression of tight junction proteins in isolated cerebral microvessels from yearling and adult sheep. Neuroimmunomodulation **20:**264–273. http://dx.doi.org/10.1159/000350470.
47. **Greenberg JI, Shields DJ, Barillas SG, Acevedo LM, Murphy E, Huang J, Scheppke L, Stockmann C, Johnson RS, Angle N, Cheresh DA.** 2008. A role for VEGF as a negative regulator of pericyte function and vessel maturation. Nature **456:**809–813. http://dx.doi.org/10.1038/nature07424.
48. **Yu VL, Hansen DS, Ko WC, Sagnimeni A, Klugman KP, von Gottberg A, Goossens H, Wagener MM, Benedi VJ.** 2007. Virulence characteristics of Klebsiella and clinical manifestations of *K. pneumoniae* bloodstream infections. Emerg. Infect. Dis. **13:**986–993. http://dx.doi.org/10.3201/eid1307.070187.
49. **Luck SN, Bennett-Wood V, Poon R, Robins-Browne RM, Hartland EL.** 2005. Invasion of epithelial cells by locus of enterocyte effacement-negative enterohemorrhagic Escherichia coli. Infect. Immun. **73:**3063–3071. http://dx.doi.org/10.1128/IAI.73.5.3063-3071.2005.
50. **Finlay BB, Rosenshine I, Donnenberg MS, Kaper JB.** 1992. Cytoskeletal composition of attaching and effacing lesions associated with enteropathogenic Escherichia coli adherence to HeLa cells. Infect. Immun. **60:**2541–2543.
51. **Sahly H, Navon-Venezia S, Roesler L, Hay A, Carmeli Y, Podschun R, Hennequin C, Forestier C, Ofek I.** 2008. Extended-spectrum beta-lactamase production is associated with an increase in cell invasion and expression of fimbrial adhesins in Klebsiella pneumoniae. Antimicrob. Agents Chemother. **52:**3029–3034. http://dx.doi.org/10.1128/AAC.00010-08.